1	Table of Contents	
2	Figure S1. PNI in PDAC patients correlates with lactylation of primary cells.	2
3	Figure S2. Lactate promotes proliferation, migration and neural tropism of PDAC cells.	4
4	Figure S3. Effect of NSUN2 in PNI of pancreatic cancer cells.	6
5	Figure S4. Quantification of NSUN2 protein and lactylation under various treatments.	8
6	Figure S5. NSUN2-K692 mutation is associated with PNI.	9
7	Figure S6. CDCP1/STC1 is associated with PNI.	12
8	Figure S7. NSUN2 K692 lactylation stabilizes CDCP1/STC1 and promotes PNI.	14
9	Figure S8. Quantification of immunofluorescence in vivo experiments related to PNI.	16
10	Table S1. Primers, probes and oligonucleotides used in the study.	18
11	Table S2. Clinical and pathologic variables	20
12	Table S3. Antibody and Kit	21
13	Table S4 Univariate and multivariate analysis of Overall Survival (OS) in PDAC patients	
14	(n = 142)	22
15	Table S5 Univariate and multivariate analysis of Disease-free Survival (DFS) in PDAC patient	ts
16	(n = 142)	23
17		
18		

Figure S1. PNI in PDAC patients correlates with lactylation of primary cells.

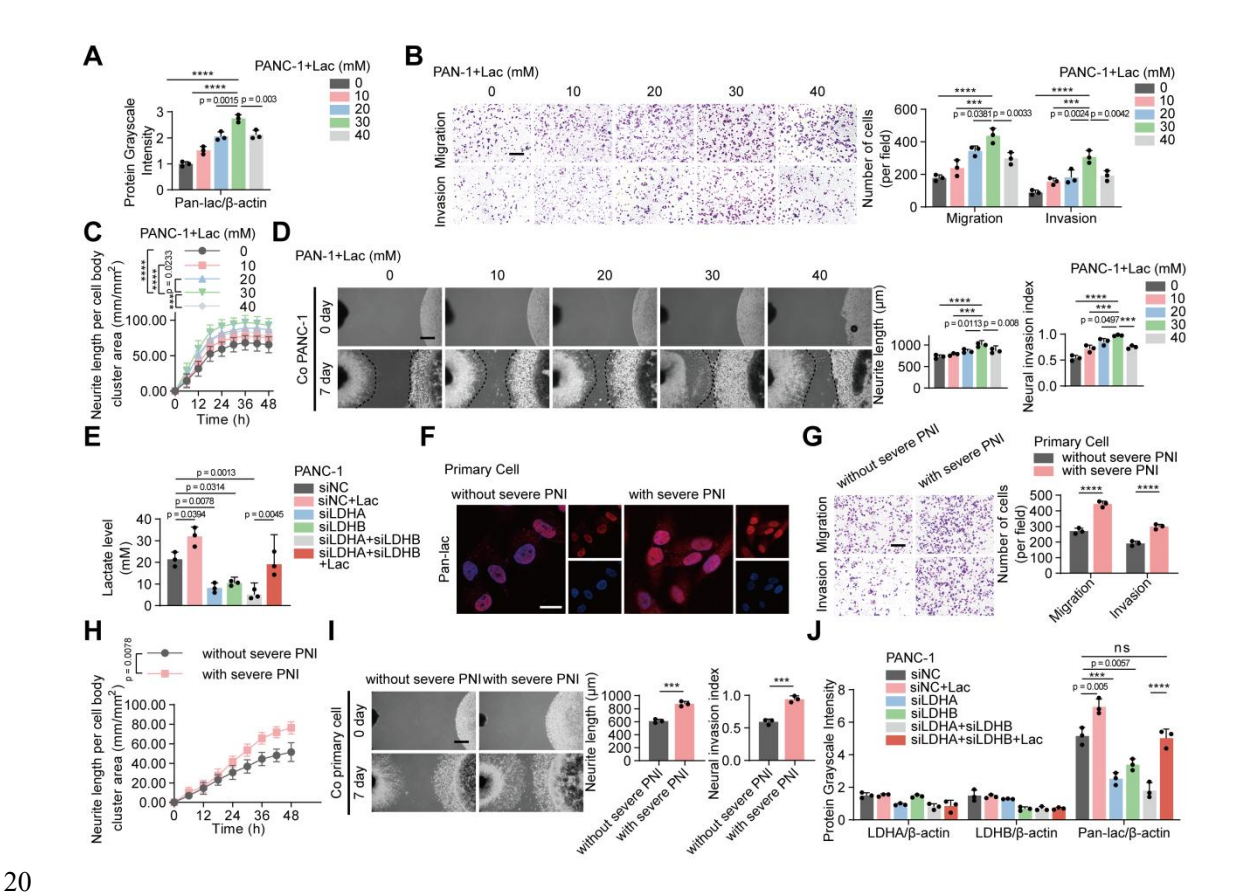


Figure S1. PNI in PDAC patients correlates with lactylation of primary cells.

21

22 (A) Quantification of lactylation intensity normalized to β -actin. (B-D) PANC-1 cells treated with 23 varying concentrations of lactate (0, 10, 20, 30, and 40 mM) for subsequent experiments. (B) PANC-1 24 Transwell migration/invasion: image panels (left) and measurements (right). Scale bar, 200 μm. (C) 25 Neurite outgrowth was quantified under the indicated conditions in the Transwell co-culture model. 26 Phase-contrast images were obtained at 6 h intervals. (D) (left) Representative fields from DRG 27 co-cultures with tumor cells. (right) Summary statistics for tumor neurite invasion toward DRG. The 28 black dashed line on the left indicates the growth boundary of the DRG, which on the right marks the 29 growth boundary of PANC-1 cells. Scale bar, 500 µm. (E) Measurement of lactate concentration in 30 PANC-1 cells after LDHA and LDHB silencing and addition of L-lactate. (F) Immunofluorescence 31 staining for Pan-lac in primary tumor cells isolated from patients grouped by PNI severity. Scale bar, 32 20 μm. (G-I) Primary tumor cells were isolated from patients grouped by PNI severity and were used 33 for subsequent experiments. (G) Primary tumor cells Transwell migration/invasion: image panels (left) 34 and measurements (right). Scale bar, 200 µm. (H) Neurite outgrowth was quantified under the indicated 35 conditions in the Transwell co-culture model. Phase-contrast images were obtained at 6 h intervals. (I) 36 (left) Representative fields from DRG co-cultures with tumor cells. (right) Summary statistics for 37 tumor neurite invasion toward DRG. Scale bar, 500 µm. (J) Densitometric analysis of protein 38 lactylation levels in PANC-1 cells following LDHA and LDHB knockdown and L-lactate 39 supplementation, as determined by immunoblot. Each experiment was performed independently in 40 triplicate, and all quantitative results are presented as mean ± SD. Statistical tests used for each panel 41 were as follows: (A, B, D, E) one-way ANOVA; (C) two-way ANOVA; (G, I) unpaired t test; (H) 42 paired t test. * for $P \le 0.05$, ** for $P \le 0.01$, *** for $P \le 0.001$ and **** for $P \le 0.0001$.

43 Figure S2. Lactate promotes proliferation, migration and neural tropism of PDAC cells.

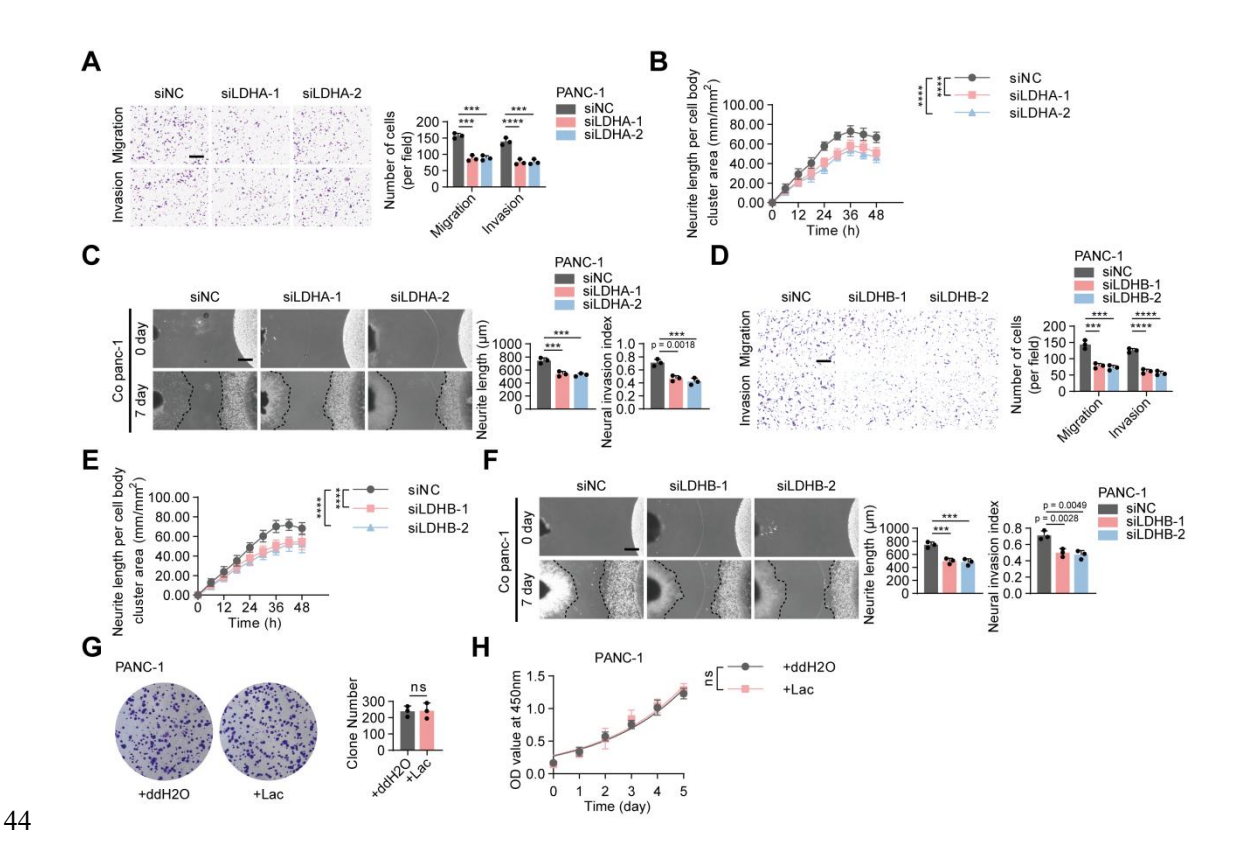


Figure S2. Lactate promotes proliferation, migration and neural tropism of PDAC cells.

45

46

47

48

49

50

51

52

53

54

55

56

57

58

59

60

61

62

(A-C) PANC-1 cells expressing LDHA siRNA or siNC were used for subsequent experiments. (A) PANC-1 Transwell migration/invasion: image panels (left) and measurements (right). Scale bar, 200 μm. (B) Neurite outgrowth was quantified under the indicated conditions in the Transwell co-culture model. Phase-contrast images were obtained at 6 h intervals. (C) (left) Representative fields from DRG co-cultures with tumor cells. (right) Summary statistics for tumor neurite invasion toward DRG. Scale bar, 500 µm. (D-F) PANC-1 cells expressing LDHB siRNA or siNC were used for subsequent experiments. (D) PANC-1 Transwell migration/invasion: image panels (left) and measurements (right). Scale bar, 200 µm. (E) Neurite outgrowth was quantified under the indicated conditions in the Transwell co-culture model. Phase-contrast images were obtained at 6 h intervals. (F) (left) Representative fields from DRG co-cultures with tumor cells. (right) Summary statistics for tumor neurite invasion toward DRG. Scale bar, 500 µm. (G) Representative images and quantitative analysis of colony formation in PANC-1 cells treated with ddH₂O or L-lactate. (H) CCK-8 assay showing the proliferation of PANC-1 cells exposed to ddH₂O or L-lactate treatment over a period of 5 days. Each experiment was performed independently in triplicate, and all quantitative results are presented as mean ± SD. Statistical tests used for each panel were as follows: (A-D, F) one-way ANOVA; (E) two-way ANOVA; (G) unpaired t test; (H) paired t test. * for $P \le 0.05$, ** for $P \le 0.01$, *** for $P \le 0.01$, *** 0.001 and **** for $P \le 0.0001$.

63 Figure S3. Effect of *NSUN2* in PNI of pancreatic cancer cells.

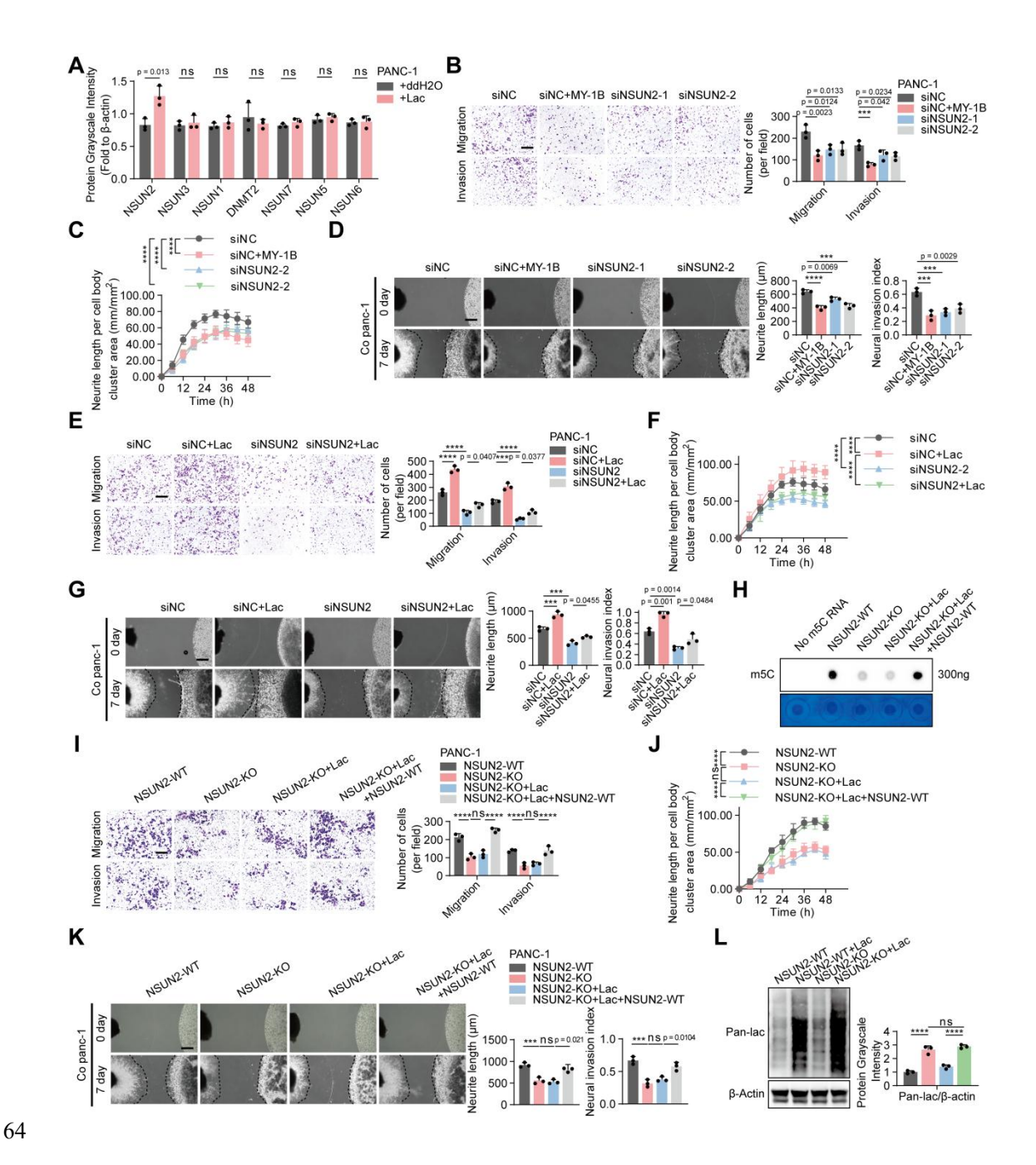


Figure S3. Effect of *NSUN2* in PNI of pancreatic cancer cells.

65

66 (A) Densitometric analysis of NSUN1, NSUN2, NSUN3, NSUN5, NSUN6, NSUN7 and DNMT2 protein 67 expression levels in PANC-1 cells with or without L-lactate treatment by Western blot. (B-D) PANC-1 68 cells expressing NSUN2 siRNA or siNC, or treatment with the NSUN2 small-molecule inhibitor 69 MY-1B for subsequent experiments. (B) PANC-1 Transwell migration/invasion: image panels (left) and 70 measurements (right). Scale bar, 200 µm. (C) Neurite outgrowth was quantified under the indicated 71 conditions in the Transwell co-culture model. Phase-contrast images were obtained at 6 h intervals. (D) 72 (left) Representative fields from DRG co-cultures with tumor cells. (right) Summary statistics for 73 tumor neurite invasion toward DRG. Scale bar, 500 µm. (E-G) PANC-1 cells expressing siNC or 74 NSUN2-specific siRNA, followed by treatment with or without L-lactate. (E) PANC-1 Transwell 75 migration/invasion: image panels (left) and measurements (right). Scale bar, 200 µm. (F) Neurite 76 outgrowth was quantified under the indicated conditions in the Transwell co-culture model. 77 Phase-contrast images were obtained at 6 h intervals. (G) (left) Representative fields from DRG 78 co-cultures with tumor cells. (right) Summary statistics for tumor neurite invasion toward DRG. Scale 79 bar, 500 µm. (H) m5C dot blot analysis of m5C levels in RNA extracted from PANC-1 cells. Methylene 80 blue staining (below) was used to detect input RNA, while the intensity of the dot blot signal (above) 81 represents the level of m5C modification. (I) PANC-1 Transwell migration/invasion: image panels (left) 82 and measurements (right). Scale bar, 200 µm. (J) Neurite outgrowth was quantified under the indicated 83 conditions in the Transwell co-culture model. Phase-contrast images were obtained at 6 h intervals. (K) 84 (left) Representative fields from DRG co-cultures with tumor cells. (right) Summary statistics for 85 tumor neurite invasion toward DRG. Scale bar, 500 µm. (L) Lactylation modification levels were 86 detected in PANC-1 cells by Western blot. Each experiment was performed independently in triplicate, 87 and all quantitative results are presented as mean ± SD. Statistical tests used for each panel were as 88 follows: (A, B, D, E, G, I, K) one-way ANOVA; (C, F, J) two-way ANOVA; (L) unpaired t test. * for 89 $P \le 0.05$, ** for $P \le 0.01$, *** for $P \le 0.001$ and **** for $P \le 0.0001$.

Figure S4. Quantification of NSUN2 protein and lactylation under various treatments.

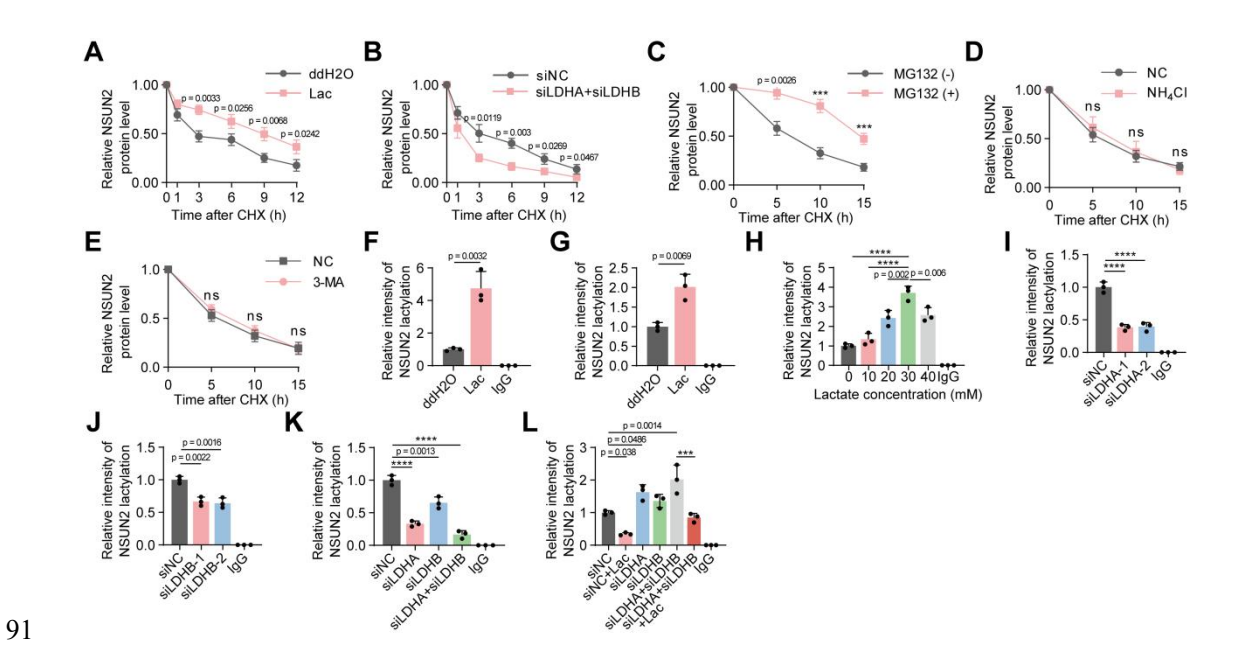


Figure S4. Quantification of NSUN2 protein and lactylation under various treatments.

(A) Quantitative analysis of *NSUN2* protein expression levels at different time points under ddH2O or L-lactate treatment. (B) Quantitative analysis of *NSUN2* protein expression levels at different time points under transfection of siNC or *LDHA/B* siRNAs treatment. (C) Quantitative analysis of *NSUN2* protein expression levels at different time points with or without MG132 treatment. (D-E) Quantitative analysis of *NSUN2* protein expression levels at different time points under NH₄Cl (D) or 3-MA (E) treatment. (F-G) Quantification of *NSUN2* lactylation intensity normalized to Flag-*NSUN2* in 293T cells (F) or PANC-1 cells (G). (H) Quantification of *NSUN2* lactylation intensity normalized to Flag-*NSUN2* under different lactate concentration treatment. (I-L) Quantification of *NSUN2* lactylation intensity normalized to Flag-*NSUN2* expressing siNC or *LDHA/B* siRNAs exposed to ddH2O or L-lactate treatment. Each experiment was performed independently in triplicate, and all quantitative results are presented as mean \pm SD. Statistical tests used for each panel were as follows: (A-G) unpaired t test; (H-L) one-way ANOVA. * for P \leq 0.05, ** for P \leq 0.01, *** for P \leq 0.001 and **** for P \leq 0.0001.

106 Figure S5. NSUN2-K692 mutation is associated with PNI.

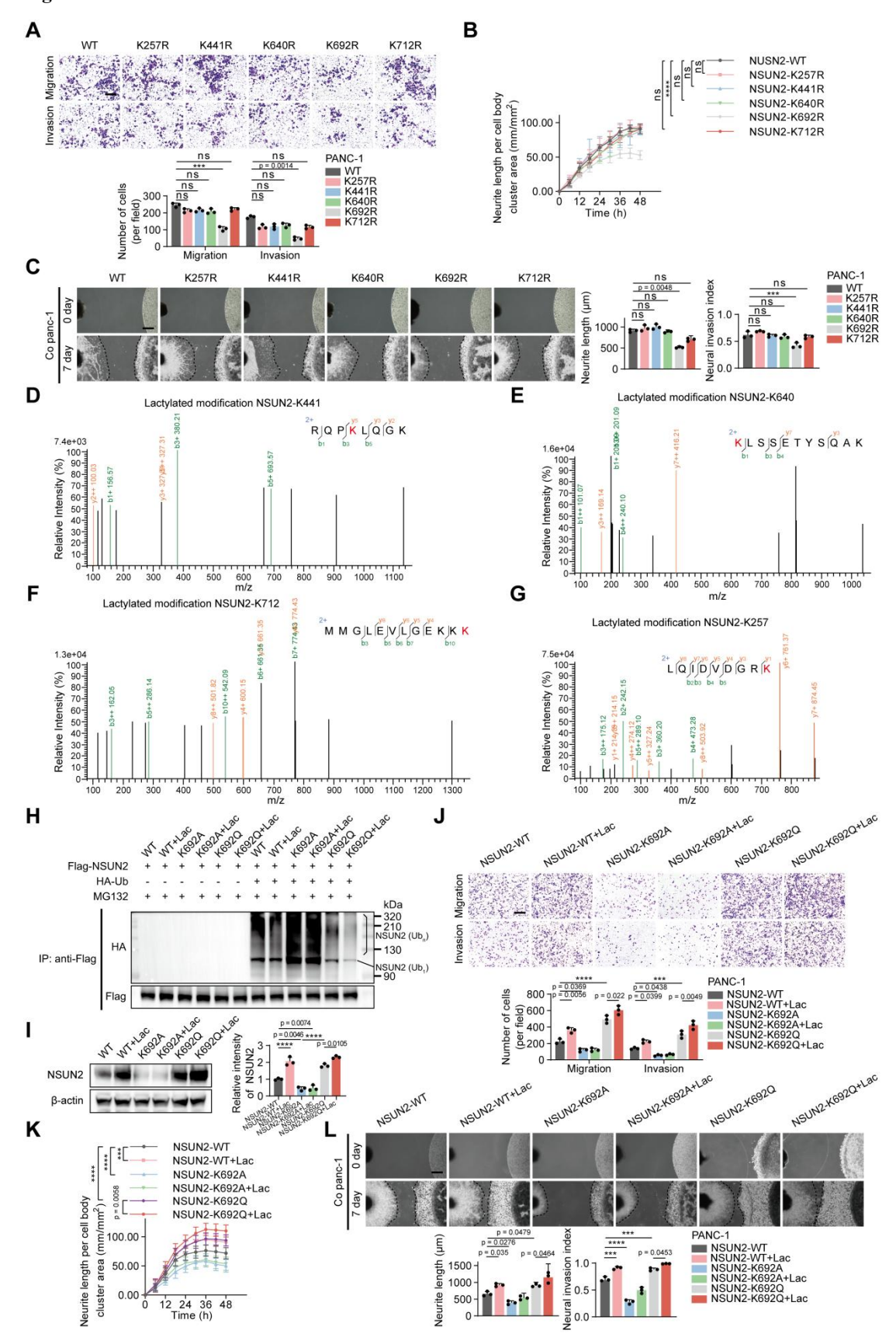


Figure S5. NSUN2-K692 mutation is associated with PNI.

108

109 (A-C) PANC-1 cells expressing indicated NSUN2 site mutations plasmids were used for subsequent 110 experiments. (A) PANC-1 Transwell migration/invasion: image panels (above) and measurements 111 (below). Scale bar, 200 µm. (B) Neurite outgrowth was quantified under the indicated conditions in the 112 Transwell co-culture model. Phase-contrast images were obtained at 6 h intervals. (C) (left) 113 Representative fields from DRG co-cultures with tumor cells. (right) Summary statistics for tumor 114 neurite invasion toward DRG. Scale bar, 500 µm. (D-G) Lactylation sites include (D) K441, (E) K640, 115 (F) K712 and (G) K257. (H-K) NSUN2-K692 mutant PANC-1 cells were generated using the CRISPR 116 / Cas9 approach. Residue K692 was replaced by alanine (K692A) or glutamine (K692Q). (H) Lysates 117 from treated PANC-1 cells were SDS-pretreated, immunoprecipitated with anti-FLAG, and probed for 118 NSUN2 ubiquitination by Western blot. The line labeled 'NSUN2 (Ub1)' indicates mono-ubiquitinated 119 NSUN2, while the bracket labeled 'NSUN2 (Ubn)' marks high molecular weight polyubiquitinated 120 NSUN2 species. (I) (Left) NSUN2 levels were detected in PANC-1 cells by Western blot. (Right) 121 Quantification of NSUN2 intensity normalized to β -actin. (J) PANC-1 Transwell migration/invasion: 122 image panels (above) and measurements (below). Scale bar, 200 µm. (K) Neurite outgrowth was 123 quantified under the indicated conditions in the Transwell co-culture model. Phase-contrast images 124 were obtained at 6 h intervals. (L) (top) Representative fields from DRG co-cultures with tumor cells. 125 (bottom) Summary statistics for tumor neurite invasion toward DRG. Scale bar, 500 µm. Each 126 experiment was performed independently in triplicate, and all quantitative results are presented as 127 mean ± SD. Statistical tests used for each panel were as follows: (A, C, I-L) one-way ANOVA; (B) 128 two-way ANOVA. * for $P \le 0.05$, ** for $P \le 0.01$, *** for $P \le 0.001$ and **** for $P \le 0.0001$.

Figure S6. *CDCP1/STC1* is associated with PNI.

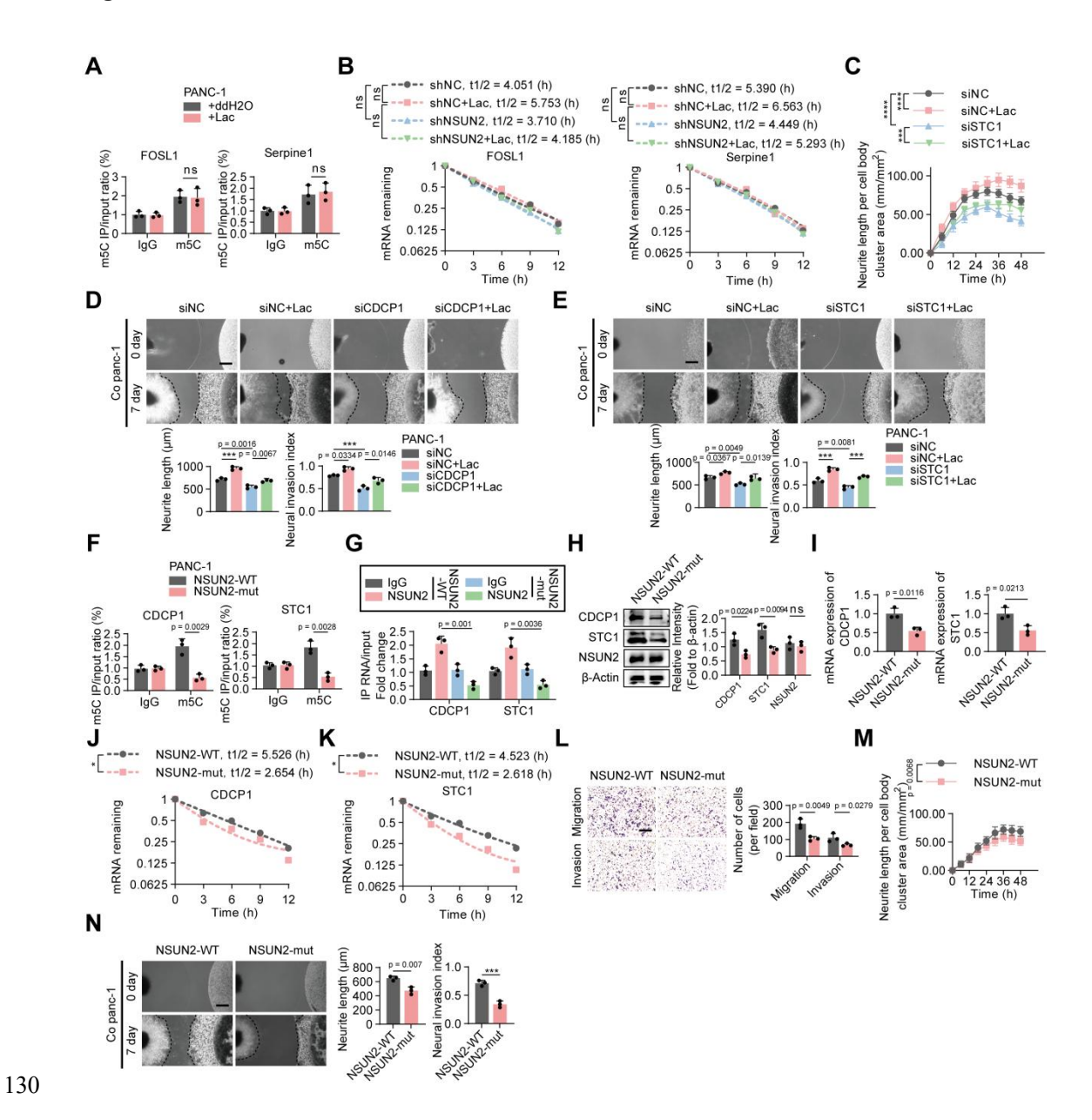


Figure S6. CDCP1/STC1 is associated with PNI.

131

132 (A) MeRIP-qPCR confirmed m5C enrichment of FOSL1 and Serpine1 transcripts in PANC-1 cells ± 133 L-lactate. (B) Actinomycin D assay to assess the half-life of FOSL1 and Serpine1 mRNA in PANC-1 134 cells expressing shNC or NSUN2-specific shRNA, followed by exposing to ddH2O or L-lactate 135 treatment. (C) Neurite outgrowth was quantified under the indicated conditions in the Transwell 136 co-culture model. Phase-contrast images were obtained at 6 h intervals. (D) (top) Representative fields 137 from DRG co-cultures with tumor cells. (bottom) Summary statistics for tumor neurite invasion toward 138 DRG. Scale bar, 500 µm. (E) (top) Representative fields from DRG co-cultures with tumor cells. 139 (bottom) Summary statistics for tumor neurite invasion toward DRG. Scale bar, 500 µm. (F-N) 140 PANC-1 cells were expressing vector or NSUN2 methylation domain mutant plasmid. (F) 141 MeRIP-qPCR analysis of CDCP1 and STC1 mRNA in the m5C peak regions in tumor cells expressing 142 either wild-type NSUN2 or NSUN2 with a mutated methylation domain. (G) CLIP assays confirmed the 143 interaction strength between NSUN2 and the indicated mRNA in PANC-1 cells expressing either 144 NSUN2-WT or NSUN2 with a mutated methylation domain. (H) Immunoblot analysis of NSUN2, 145 CDCP1 and STC1 protein expression levels in PANC-1 cells under the indicated treatments. (I) Total 146 RNA isolated from treated PANC-1 cells was used for qRT-PCR analysis to assess the CDCP1 and 147 STC1 mRNA expression. (J-K) Actinomycin D assay to assess the half-life of CDCP1 (J) and STC1 (K) 148 mRNA in tumor cells. (L) PANC-1 Transwell migration/invasion: image panels (left) and 149 measurements (right). Scale bar, 200 µm. (M) Neurite outgrowth was quantified under the indicated 150 conditions in the Transwell co-culture model. Phase-contrast images were obtained at 6 h intervals. (N) 151 (left) Representative fields from DRG co-cultures with tumor cells. (right) Summary statistics for 152 tumor neurite invasion toward DRG. Scale bar, 500 µm. Each experiment was performed 153 independently in triplicate, and all quantitative results are presented as mean ± SD. Statistical tests used 154 for each panel were as follows: (D, E, H) one-way ANOVA; (C) two-way ANOVA; (L, N) unpaired t test; (M) paired t test. * for $P \le 0.05$, ** for $P \le 0.01$, *** for $P \le 0.001$ and *** for $P \le 0.0001$. 155

Figure S7. NSUN2 K692 lactylation stabilizes CDCP1/STC1 and promotes PNI.

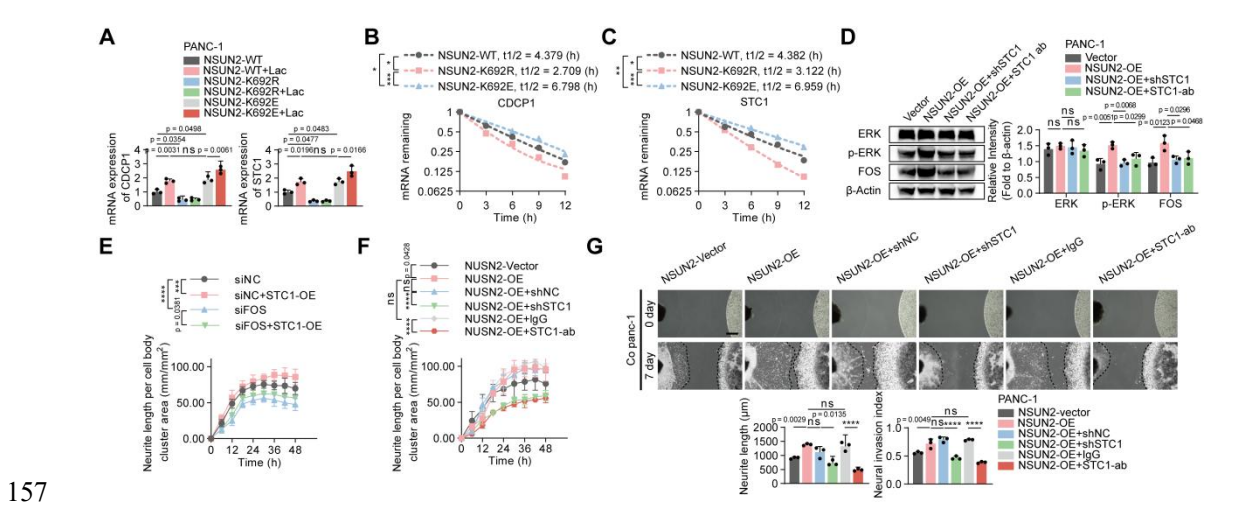


Figure S7. NSUN2 K692 lactylation stabilizes CDCP1/STC1 and promotes PNI.

158

159

160

161

162

163

164

165

166

167

168

169

170

171

172

173

174

175

176

(A) PANC-1 cells harboring the NSUN2-K692R or NSUN2-K692E mutant were generated using the CRISPR / Cas9 system, followed by treatment with or without L-lactate. Total RNA was extracted and subjected to qRT-PCR to assess the mRNA expression levels of CDCP1 and STC1. (B-C) Actinomycin D assay to assess the half-life of CDCP1 (B) and STC1 (C) mRNA in PANC-1 cells. (D) Immunoblot analysis (left) and quantification analysis (right) of ERK / FOS signaling pathway in PANC-1 cells expressing vector or NSUN2 overexpression plasmid, followed by treatment with or without transfection with STC1 shRNA or STC1 neutralizing antibody. (E) Neurite outgrowth was quantified under the indicated conditions in the Transwell co-culture model. The PANC-1 cells expressing siNC or FOS siRNA, followed by exposing to transfecting with STC1 overexpression plasmid treatment. Phase-contrast images were obtained at 6 h intervals. (F-G) PANC-1 cells were expressing NSUN2-OE plasmid, followed by \pm shSTCI and \pm STCI-neutralizing antibody (isotype control), and subjected to subsequent experiments. (F) Neurite outgrowth was quantified under the indicated conditions in the Transwell co-culture model. Phase-contrast images were obtained at 6 h intervals. (G) (top) Representative fields from DRG co-cultures with tumor cells. (bottom) Summary statistics for tumor neurite invasion toward DRG. Scale bar, 500 µm. Each experiment was performed independently in triplicate, and all quantitative results are presented as mean \pm SD. Statistical tests used for each panel were as follows: (D, G) one-way ANOVA; (E, F) two-way ANOVA. * for $P \le 0.05$, ** for $P \le 0.01$, *** for $P \le 0.001$ and **** for $P \le 0.0001$.

177 Figure S8. Quantification of immunofluorescence in vivo experiments related to PNI.

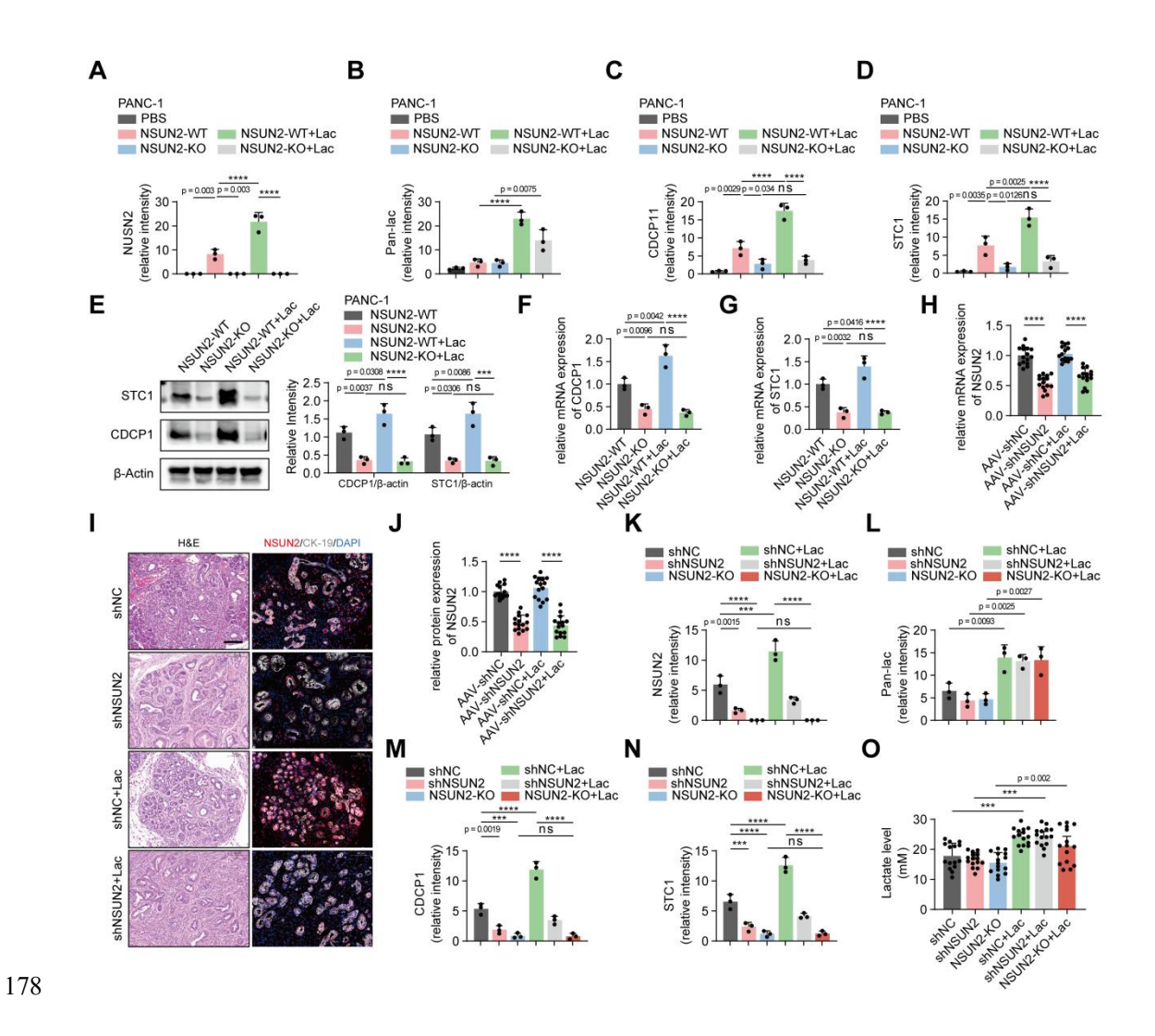


Figure S8. Quantification of immunofluorescence in vivo experiments related to PNI.

(A-D) Quantification of mIF images showing *NSUN2* (A), Pan-lac (B), *CDCP1* (C) and *STC1* (D) expression in sciatic nerve invasion model mice. (E) Immunoblot analysis (left) and quantification analysis (right) of *STC1* and *CDCP1* in tumor lysates from the sciatic-nerve invasion mouse model. (F-G) RT-qPCR analysis of *CDCP1* (F) and *STC1* (G) mRNA in tumor lysates from the sciatic-nerve invasion mouse model. (H-O) Following orthotopic AAV-mediated delivery of shNSUN2 in KPC mice with or without L-lactate treatment, tumor tissues were collected for subsequent experiments. (H) RT-qPCR quantification of *NSUN2* mRNA in tumors. (I-J) Immunofluorescence staining and quantification of *NSUN2* and *CK19* in tumors. (K-N) Quantification of mIF images showing *NSUN2* (K), Pan-lac (L), *CDCP1* (M) and *STC1* (N) expression in KPC model mice. (O) Lactate concentration in tumor tissues. Experiments shown in panels A-G and K-N were independently in triplicate (n = 3), whereas those in panels H-J and O involved fifteen biological replicates (n = 15), and all quantitative results are presented as mean \pm SD. Statistical tests used for each panel were as follows: (A-O) one-way ANOVA. * for P \leq 0.05, ** for P \leq 0.01, *** for P \leq 0.001 and **** for P \leq 0.0001.

Table S1. Primers, probes and oligonucleotides used in the study.

1	94	
1	95	

ne	Sequence(5'-3')	Application		
<i>NSUN2</i> -F	CAAGCTGTTCGAGCACTACTAC	qRT-PCR		
<i>NSUN2-</i> R	CTCCCTGAGAGCGTCCATGA			
CDCP1-F	CTGAACTGCGGGGTCTCTATC	qRT-PCR		
CDCP1-R	GTCCCCAGCTTTATGAGAACTG	-		
STC1-F	GTGGCGGCTCAAAACTCAG	qRT-PCR		
STC1-R	GTGGAGCACCTCCGAATGG	_		
<i>GAPDH</i> -F	ACAACTTTGGTATCGTGGAAGG	qRT-PCR		
<i>GAPDH</i> -R	GCCATCACGCCACAGTTTC			
<i>NSUN5</i> -F	CGCTACCATGAGGTCCACTAC	qRT-PCR		
<i>NSUN5</i> -R	GCATCTCGCACCACGTCTT			
<i>NSUN6</i> -F	TTAAGAGGAGCCCATGTCTATGC	qRT-PCR		
<i>NSUN6</i> -R	CTTTGCGGCTTAGTTCAGAAATC			
<i>NSUN7-</i> F	GCATTGGCAAGATGTCGAATC	qRT-PCR		
NSUN7-R	GGCCCTTAGTTCCTGTTTCCTA			
FOSL1-F	CAGGCGGAGACTGACAAACTG	qRT-PCR		
FOSL1-R	TCCTTCCGGGATTTTGCAGAT			
Serpine1-F	ACCGCAACGTGGTTTTCTCA	qRT-PCR		
Serpine1-R	TTGAATCCCATAGCTGCTTGAAT			
si/shNSUN2-1-sense	CGAAUGAUGUGGACAACAA	siRNA/shRNA		
si/shNSUN2-1-antisense	UUGUUGUCCACAUCAUUCG			
si/shNSUN2-2-sense	CAGUUUCUAGUUAGUGAAA	siRNA/shRNA		
si/shNSUN2-2-antisense	UUUCACUAACUAGAAACUG			
siSTC1-sense	GGAUGUAUGACAUCUGUAAtt	siRNA		
siSTC1-antisense	UUACAGAUGUCAUACAUCCtt			
siCDCP1-sense	CCACGAGAAAGCAACAUUAtt	siRNA		
siCDCP1-antisense	UAAUGUUGCUUUCUCGUGGtt			
siLDHA-1-sense	GCUGAUUUAUAAUCUUCUAtt	siRNA		
siLDHA-1-antisense	UAGAAGAUUAUAAAUCAGCtt			
siLDHA-2-sense	GAAGAAGAGUGCAGAUACAtt	siRNA		
siLDHA-2-antisense	UGUAUCUGCACUCUUCUUCtt			
siLDHB-1-sense	GGUUGCUCAGCUCAAGAAAtt	siRNA		
siLDHB-1-antisense	UUUCUUGAGCUGAGCAACCtt			
siLDHB-2-sense	GGUUGAAAGUGCCUAUGAAtt	siRNA		
siLDHB-2-antisense	UUCAUAGGCACUUUCAACCtt			
sgRNA-S1 (K692)	CGCCATCCGCATAAGACGAT	CRISPR-Cas9 geno editing (sgRNA)		
sgRNA-S2 (K692)	CCGCCATCCGCATAAGACGA	CRISPR-Cas9 geno editing (sgRNA)		
sgRNA-S3 (K692)	CCATCGTCTTATGCGGATGG	CRISPR-Cas9 geno editing (sgRNA)		
ssODN-E (K692E)	ACGCTCTGCAGTGTCCCATCGTCTTATGC	UDD rongin tone 1-4		
	GGATGGCGGGAAAGGCCTCCATTCGAACTT	HDR repair templat (ssODN donor)		
	TTGTGCCCGAGAATGAACGGCTTCATTATCTC	()		
	AGGATGATGGGGCTGGAGGTATTGGGAGAAA			
	AGAAGAAGGAAG			

ssODN-R (K692R)	ACGCTCTGCAGTGTCCCATCGTCTTATGC GGATGGCGGGGAAAGGCCTCCATTCGAACTT TTGTGCCCAGAAATGAACGGCTTCATTATCTC AGGATGATGGGGCTGGAGGTATTGGGAGAAA	HDR repair template (ssODN donor)
ssODN-Q (K692Q)	AGAAGAAGGAAG ACGCTCTGCAGTGTCCCATCGTCTTATGC GGATGGCGGGGAAAGGCCTCCATTCGAACTT TTGTGCCCCAGAATGAACGGCTTCATTATCTC AGGATGATGGGGCTGGAGGTATTGGGAGAAA AGAAGAAGAAG	HDR repair template (ssODN donor)
ssODN-A (K692A)	ACGCTCTGCAGTGTCCCATCGTCTTATGC GGATGGCGGGGAAAGGCCTCCATTCGAACTT TTGTGCCCGCGAATGAACGGCTTCATTATCTC AGGATGATGGGGCTGGAGGTATTGGGAGAAA AGAAGAAGGAAG	HDR repair template (ssODN donor)
NSUN2-geno-F	AAGGACCTGGCAAAGGGAAG	PCR genotyping/ Sanger validation
NSUN2-geno-R	ACGTCATTGTCTGGCTGTCC	_
sgRNA (Exon 7)	TCTTGGCTTGATGGACGAGC	CRISPR-Cas9 RNP
ssODN (Exon 7)	AGGGATTTGTTATTGCGAATGATGTGGAC AACAAGCGCTGCTATCCTGCTCGTCCATCAAG CCAAGAGGCTGAGCAGCCCCTGCATCATGGT GGTCAACCATGATGCCTCCAGCATACCCAGGC	HDR donor
	TCCAGATAGA	DCD to 1
NSUN2-geno-F	CCTGGCTCAAAGACCACACA	PCR genotyping/ Sanger validation
NSUN2-geno-R	CTCTTTCCTGCCGTCCACAT	C
No m5C RNA (control)	AUGCAGUACGUAGCUGAUACGUCAG UCGACGUAGCUAGUCGAUCGUACGAUGC UAGUCGAUCGACGUCAGUCGAUGCAGUA CCGUAUGCUAGCUGAUCGUAGCUGAUCG ACGUAGCUGACGUAGCUGAUCGAC GUAGCUGAUCGACGUCGAUCGACG UAG	Negative control RNA (dot blot specificity)

Table S2. Clinical and pathologic variables

Clinical variables				
Age, median (range), year		59.73 (37-79)		
Gender, male/female, male%		86/56, 60.56%		
Preoperative CEA, median (range), ng/r	mL	7.06 (0.20-314.50)		
Preoperative CA19–9, median (range),	U/mL	450.82 (0.60-6816.00) 21/121, 14.79%		
Survival Status, survival/dead, survival	%			
Pathologic variables				
Histology differentiations, caes (%)				
	Well	11 (7.75)		
	Moderate	65 (45.77)		
	Poor	66 (46.48)		
T stage, cases (%)				
	T1	9 (6.34)		
	T2	12 (8.45)		
	Т3	121 (85.21)		
ΓΝM stage, cases (%)				
	IA	6 (4.23)		
	IB	7 (4.93)		
	IIA	48 (33.80)		
	IIB	81 (57.04)		
.ymph_Node (+), cases (%)		81 (57.04)		
Perineural_Invasion (+), cases (%)		116 (81.69)		

Table S3. Antibody and Kit

Company	Antibody	Art.No.	Species	Application and Dilution		
Immunofluorescence Antibody						
Jingjie	Anti-L-Lactyl Lysine Rabbit mAb	PTM-1401RM	Rabbit	WB 1:500-1:1000	IHC-P 1:50-1:100	ICC/IF 1:50-1:100
CST	β3-Tubulin	D65A4	Rabbit	WB 1:1000	IHC-P 1:50	IP 1:50
CST	Keratin 17/19	D4G2	Rabbit	WB 1:1000	IHC-P 1:1200	IF 1:50
abcam	STUB1	ab134064	Rabbit	WB 1:10000-1:50000	IHC-P 1:100	IF/ICC 1:250-1:500
proteintech	NSUN2	20854-1-AP	Rabbit	WB 1:5000-1:50000	IHC-P 1:50-1:500	IF/ICC 1:750-1:300
proteintech	CDCP1	12754-1-AP	Rabbit	WB 1:500-1:2000	IHC-P 1:50-1:500	
proteintech	STCI	20621-1-AP	Rabbit	WB 1:500-1:1000	IHC-P 1:50-1:500	
Western blotting Antibody						
proteintech	B-Actin	20536-1-AP	Rabbit	WB 1:4000-1:10000	IHC-P 1:50-1:500	IF/ICC 1:200-1:800
proteintech	NSUN5	15449-1-AP	Rabbit	WB 1:500-1:3000	IHC-P 1:50-1:500	
proteintech	NSUN6	17240-1-AP	Rabbit	WB 1:500-1:2000	IHC-P 1:500-1:2000	
proteintech	ubiquitin	10201-2-AP	Rabbit	WB 1:1000-1:8000	IHC-P 1:50-1:500	IF/ICC 1:200-1:800
proteintech	5-methylcytosine	68301-1-Ig	Mouse	Dot Blot 1:2500-1:10000	IHC-P 1:2500-1:10000	
proteintech	ERK1/2	11257-1-AP	Rabbit	WB 1:2000-1:16000		
proteintech	Phospho-ERK1/2	80031-1-RR	Rabbit	WB 1:2000-1:10000		
proteintech	c-Fos	66590-1-Ig	Mouse	WB 1:5000-1:50000		
UpingBio	NSUN7	YP-Ab-11882	Rabbit	WB 1:500-1:2000		
Immunoprecipitation Antibody						
abcam	NSUN2	ab259941	Rabbit	IP 1:30	IHC-P 1:200	ICC/IF 1:1000
abcam	5-methylcytosine	ab10805	Mouse	IP 1:50		
CST	DYKDDDDK Tag	D6W5B	Rabbit	WB 1:1000	IHC-P 1:400-1:1600	IP 1:50
CST	HA-Tag	C29F4	Rabbit	WB 1:1000	IHC-P 1:800-1:3200	IP 1:50
Kit						
Vazyme, China	PrimeScript RT Reagent Kit					
Panovue, China	PANO 4-plex IHC Kit					
EZB Bioscience, USA	Universal RNA Purification Kit					
Millipore, USA	EZ-Magna RIP kit					
Ambion, USA Solarbio, China	Dynabeads mRNA Purification Kit Lactate Assay Kit					

Table S4 Univariate and multivariate analysis of Overall Survival (OS) in PDAC patients (n = 142)

Variables	Characteristics	Univariate analysis			Multivariate analysis		
		HR 95% CI p value		p value	HR	95% CI	p value
Age	< 60 (ref)						
	≥ 60	1.013	0.846-1.214	0.886			
Gender	Female (ref)						
	Male	1.027	0.854-1.235	0.779			
Differentiation	Well (ref)						
	Moderate	1.219	0.856-1.736	0.273	0.983	0.687-1.406	0.923
	Poor	2.184	1.532-3.112	<0.001***	1.776	1.222-2.58	0.003**
TNM stage	I (ref)						
	II	3.899	1.933-7.864	<0.001***	3.061	1.479-6.336	0.003**
T stage	I (ref)						
	II	1.246	0.759-2.045	0.385			
	III	1.464	1.005-2.133	0.047*			
Lymph node metastasis	Negative (ref)						
	Positive	2.012	1.375-2.946	<0.001***			
Perineural invasion	Negative (ref)						
	Positive	2.195	1.602-3.008	<0.001***	1.421	1.012-1.994	0.043*

Abbreviations: HR = hazard ratio; 95% CI = 95% confidence interval; TNM = tumor node metastasis; ref = reference. As lymph node metastasis and T stage are included in the TNM stage, we didn't include it in the multivariate analysis. Cox regression analysis, * p < 0.05, ** p < 0.01, *** p < 0.001.

Table S5 Univariate and multivariate analysis of Disease-free Survival (DFS) in PDAC patients (n = 142)

Variables	Characteristics	Univariate analysis			Multivariate analysis		
		HR	95% CI	p value	HR	95% CI	p value
Age	< 60 (ref)						
	≥ 60	1.013	0.847-1.213	0.885			
Gender	Female (ref)						
	Male	1.042	0.868-1.252	0.657			
Differentiation	Well (ref)						
	Moderate	1.202	0.845-1.71	0.307	1.015	0.704-1.463	0.936
	Poor	2.129	1.496-3.03	<0.001***	1.753	1.197-2.566	0.004**
TNM stage	I (ref)						
	II	4.511	2.206-9.226	<0.001***	4.013	1.833-8.784	<0.001***
T stage	I (ref)						
	II	1.222	0.744-2.005	0.429			
	III	1.515	1.04-2.206	0.03*			
Lymph node metastasis	Negative (ref)						
	Positive	2.152	1.467-3.158	<0.001***			
Perineural invasion	Negative (ref)						
	Positive	2.275	1.66-3.118	<0.001***	1.484	1.056-2.085	0.023*

Abbreviations: HR = hazard ratio; 95% CI = 95% confidence interval; TNM = tumor node metastasis; ref = reference. As lymph node metastasis and T stage are included in the TNM stage, we didn't include it in the multivariate analysis. Cox regression analysis, * p < 0.05, ** p < 0.01, *** p < 0.001.